A bottom-up approach to fabricate optical metamaterials by self-assembled metallic nanoparticles

José Dintinger,[1,*] Stefan Mühlig,[2] Carsten Rockstuhl,[2] and Toralf Scharf[1]

[1]*Optics & Photonics Technology Laboratory, Ecole Polytechnique Fédérale de Lausanne (EPFL), Neuchâtel, CH-2000, Switzerland*

[2]*Institute of Condensed Matter Theory and Solid State Optics, Abbe Center of Photonics, Friedrich-Schiller-Universität Jena, D-07743 Jena, Germany*

**jose.dintinger@epfl.ch*

Abstract: We introduce a novel bottom-up approach to fabricate by self assembly a metamaterial from metallic nanoparticles in a two-step process. In the first step, a metamaterial made of densely packed silver nanoparticles is required. The material dispersion with increasing nanoparticle densities, from dispersed to randomly packed nanoparticles, was measured by spectroscopic ellipsometry, demonstrating high permittivity values in the visible. In the second step, this material was used to prepare spherical clusters by a method based on oil-in-water emulsion. The optical properties of these clusters were equally investigated by spectroscopic means. Comparisons with rigorous numerical simulations clearly indicate that, depending on the cluster size, their spectral response can be unambiguously associated with the excitation of a magnetic dipole resonance. As a consequence, such spherical clusters are promising building blocks for future metamaterials possessing a magnetic response in the visible range.

©2012 Optical Society of America

OCIS codes: (160.3918) Metamaterials; (160.4760) Optical properties; (250.5403) Plasmonics; (290.4210) Multiple scattering.

References and links

1. W. Cai and V. Shalaev, *Optical Metamaterials Fundamentals and Applications* (Springer, 2010).
2. C. M. Soukoulis, S. Linden, and M. Wegener, "Physics. Negative refractive index at optical wavelengths," Science **315**(5808), 47–49 (2007).
3. N. I. Zheludev, "Applied physics. The road ahead for metamaterials," Science **328**(5978), 582–583 (2010).
4. J. B. Pendry, A. J. Holden, D. J. Robbins, and W. J. Stewart, "Magnetism from conductors and enhanced nonlinear phenomena," IEEE Trans. Microw. Theory Tech. **47**(11), 2075–2084 (1999).
5. S. Linden, C. Enkrich, M. Wegener, J. F. Zhou, T. Koschny, and C. M. Soukoulis, "Magnetic response of metamaterials at 100 terahertz," Science **306**(5700), 1351–1353 (2004).
6. G. Dolling, C. Enkrich, M. Wegener, J. F. Zhou, C. M. Soukoulis, and S. Linden, "Cut-wire pairs and plate pairs as magnetic atoms for optical metamaterials," Opt. Lett. **30**(23), 3198–3200 (2005).
7. V. M. Shalaev, W. S. Cai, U. K. Chettiar, H. K. Yuan, A. K. Sarychev, V. P. Drachev, and A. V. Kildishev, "Negative index of refraction in optical metamaterials," Opt. Lett. **30**(24), 3356–3358 (2005).
8. C. M. Soukoulis and M. Wegener, "Past achievements and future challenges in the development of three-dimensional photonic metamaterials," Nat. Photonics **5**, 523–530 (2011).
9. S. O'Brien and J. B. Pendry, "Photonic band-gap effects and magnetic activity in dielectric composites," J. Phys. Condens. Matter **14**(15), 4035–4044 (2002).
10. L. Lewin, "The electrical constants of a material loaded with spherical particles," Proc. Inst. Electr. Eng. **94**, 65–68 (1947).
11. L. Peng, L. Ran, H. Chen, H. Zhang, J. A. Kong, and T. M. Grzegorczyk, "Experimental observation of left-handed behavior in an array of standard dielectric resonators," Phys. Rev. Lett. **98**(15), 157403 (2007).
12. J. A. Schuller, R. Zia, T. Taubner, and M. L. Brongersma, "Dielectric metamaterials based on electric and magnetic resonances of silicon carbide particles," Phys. Rev. Lett. **99**(10), 107401 (2007).
13. R. Paniagua-Domínguez, F. López-Tejeira, R. Marqués, and J. A. Sánchez-Gil, "Metallo-dielectric core–shell nanospheres as building blocks for optical three-dimensional isotropic negative-index metamaterials," New J. Phys. **13**(12), 123017 (2011).
14. A. B. Evlyukhin, C. Reinhardt, A. Seidel, B. S. Luk'yanchuk, and B. N. Chichkov, "Optical response features of Si-nanoparticle arrays," Phys. Rev. B **82**(4), 045404 (2010).

#161083 - $15.00 USD Received 10 Jan 2012; revised 11 Feb 2012; accepted 11 Feb 2012; published 14 Feb 2012

15. V. Yannopapas, "Artificial magnetism and negative refractive index in three-dimensional metamaterials of spherical particles at near-infrared and visible frequencies," Appl. Phys., A Mater. Sci. Process. **87**(2), 259–264 (2007).
16. V. Yannopapas and A. Moroz, "Negative refractive index metamaterials from inherently non-magnetic materials for deep infrared to terahertz frequency ranges," J. Phys. Condens. Matter **17**(25), 3717–3734 (2005).
17. V. Yannopapas and N. V. Vitanov, "Photoexcitation-induced magnetism in arrays of semiconductor nanoparticles with a strong excitonic oscillator strength," Phys. Rev. B **74**(19), 193304 (2006).
18. S. Mühlig, C. Rockstuhl, V. Yannopapas, T. Bürgi, N. Shalkevich, and F. Lederer, "Optical properties of a fabricated self-assembled bottom-up bulk metamaterial," Opt. Express **19**(10), 9607–9616 (2011).
19. C. Rockstuhl, F. Lederer, C. Etrich, T. Pertsch, and T. Scharf, "Design of an artificial three-dimensional composite metamaterial with magnetic resonances in the visible range of the electromagnetic spectrum," Phys. Rev. Lett. **99**(1), 017401 (2007).
20. S. Mühlig, A. Cunningham, S. Scheeler, C. Pacholski, T. Bürgi, C. Rockstuhl, and F. Lederer, "Self-assembled plasmonic core-shell clusters with an isotropic magnetic dipole response in the visible range," ACS Nano **5**(8), 6586–6592 (2011).
21. C. R. Simovski and S. A. Tretyakov, "Model of isotropic resonant magnetism in the visible range based on core-shell clusters," Phys. Rev. B **79**(4), 045111 (2009).
22. A. Vallecchi, M. Albani, and F. Capolino, "Collective electric and magnetic plasmonic resonances in spherical nanoclusters," Opt. Express **19**(3), 2754–2772 (2011).
23. R. M. A. Azzam and N. M. Bashara, *Ellipsometry and Polarized Light* (Elsevier, 1987).
24. R. A. Synowicki, G. K. Pribil, G. Cooney, C. M. Herzinger, S. E. Green, R. H. French, M. K. Yang, J. H. Burnett, and S. Kaplan, "Fluid refractive index measurements using rough surface and prism minimum deviation techniques," J. Vac. Sci. Technol. B **22**(6), 3450–3453 (2004).
25. W. T. Doyle, "Optical properties of a suspension of metal spheres," Phys. Rev. B Condens. Matter **39**(14), 9852–9858 (1989).
26. R. Ruppin, "Evaluation of extended Maxwell-Garnett theories," Opt. Commun. **182**(4-6), 273–279 (2000).
27. P. B. Johnson and R. W. Christy, "Optical constants of noble metals," Phys. Rev. B **6**(12), 4370–4379 (1972).
28. F. Bai, D. Wang, Z. Huo, W. Chen, L. Liu, X. Liang, C. Chen, X. Wang, Q. Peng, and Y. Li, "A versatile bottom-up assembly approach to colloidal spheres from nanocrystals," Angew. Chem. Int. Ed. Engl. **46**(35), 6650–6653 (2007).
29. I. Hussain, H. Zhang, M. Brust, J. Barauskas, and A. I. Cooper, "Emulsions-directed assembly of gold nanoparticles to molecularly-linked and size-controlled spherical aggregates," J. Colloid Interface Sci. **350**(1), 368–372 (2010).
30. P. Qiu, C. Jensen, N. Charity, R. Towner, and C. Mao, "Oil phase evaporation-induced self-assembly of hydrophobic nanoparticles into spherical clusters with controlled surface chemistry in an oil-in-water dispersion and comparison of behaviors of individual and clustered iron oxide nanoparticles," J. Am. Chem. Soc. **132**(50), 17724–17732 (2010).
31. S. Mühlig, C. Rockstuhl, J. Pniewski, C. R. Simovski, S. A. Tretyakov, and F. Lederer, "Three-dimensional metamaterial nanotips," Phys. Rev. B **81**(7), 075317 (2010).
32. Y. L. Xu, "Electromagnetic scattering by an aggregate of spheres," Appl. Opt. **34**(21), 4573–4588 (1995).
33. S. Mühlig, C. Menzel, C. Rockstuhl, and F. Lederer, "Multipole analysis of meta-atoms," Metamaterials (Amst.) **5**(2-3), 64–73 (2011).
34. J. Petschulat, J. Yang, C. Menzel, C. Rockstuhl, A. Chipouline, P. Lalanne, A. Tüennermann, F. Lederer, and T. Pertsch, "Understanding the electric and magnetic response of isolated metaatoms by means of a multipolar field decomposition," Opt. Express **18**(14), 14454–14466 (2010).
35. C. Rockstuhl, C. Menzel, S. Mühlig, J. Petschulat, C. Helgert, C. Etrich, A. Chipouline, T. Pertsch, and F. Lederer, "Scattering properties of meta-atoms," Phys. Rev. B **83**(24), 245119 (2011).

1. Introduction

During the past decade, the emergence of metamaterials, as a new class of artificial materials, has triggered a wide range of new perspectives to manipulate light [1–3]. Indeed, the rational design of the metamaterial building blocks, the so-called meta-atoms, allows to tailor their electromagnetic response at will, offering unique possibilities to obtain properties inaccessible with natural materials, e.g. an effective negative index. The most challenging task to achieve full control over the light propagation characteristics is to engineer the magnetic response of the metamaterial. Several structures have been successfully implemented over the past years to tackle this problem. They are all based on subwavelength conducting inclusions with complex geometries such as metallic split rings [4,5] or cut wire pairs [6,7]. Despite these successful achievements, current metamaterials still suffer from several drawbacks which severely limit their applicability. Due to their complex architectures, their fabrication requires advanced top-down nanofabrication methods such as electron beam or ion beam lithography. Besides being expensive and time-consuming, these techniques are also generally limited to the realization of planar arrangements of meta-atoms which makes it difficult to fabricate a

#161083 - $15.00 USD Received 10 Jan 2012; revised 11 Feb 2012; accepted 11 Feb 2012; published 14 Feb 2012
(C) 2012 OSA

three dimensional bulk metamaterial in which light can effectively propagate. Additionally, this also results in anisotropic geometries suffering moreover from strong spatial dispersion due to the rather large size of the meta-atoms and their strictly periodic arrangement. In consequence the metamaterial properties are angle and polarization dependent in a highly non-trivial manner. This denies their application for many envisioned devices that have been proposed while assuming to have a material at hand with an isotropic electric and magnetic response. Finally, the operation of current metamaterials in the visible remains limited due to the difficulties to further scale down the size of the meta-atoms. Hence, the current challenge is to develop new strategies to realize three dimensional metamaterials with isotropic properties operating at optical frequencies [8]. An alternative to the metal-based metamaterials, which could potentially overcome all these limitations, is based on the excitation of resonance modes in dielectric resonators. The first order Mie mode of a dielectric sphere occurring at the smallest frequency, for instance, is known to behave as a magnetic dipole due to the resonant excitation of strong displacement currents in the sphere. Such particles could therefore be used as meta-atoms to form an effective medium with a negative permeability [9,10] provided that their size is sufficiently small to operate in the subwavelength regime. Nonetheless, this also requires a dielectric material with an extremely high permittivity. As a consequence, the excitation of such magnetic Mie resonances was first demonstrated at microwave [11] and mid infrared [12] frequencies where some high permittivity bulk materials do exist. Theoretical suggestions have also been made for the near-infrared using silicon [13,14] and for the UV-visible range using excitonic materials [15–17] but their experimental realization has not been achieved so far. Another approach that was recently investigated both theoretically and experimentally is to use metal nanoparticle (NP) composites as the precursors to form Mie resonant magnetic meta-atoms. Such meta-atoms can be formed either by arranging NPs into spherical clusters [18,19], as depicted in Fig. 1, or by decorating a dielectric core with a NP shell [20–22].

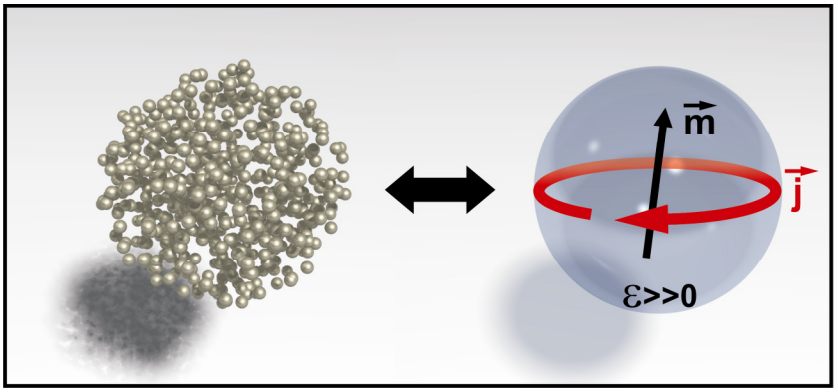

Fig. 1. A silver NP metasphere behaves as high permittivity dielectric sphere. When the first Mie resonance is excited, it acts as magnetic dipole $\vec{m}$, induced by displacement current $\vec{j}$ circulating in a plane perpendicular to the polarization of the incident magnetic field.

In both cases, the plasmonic resonances of metal NPs are at the origin of the high permittivity values sought in the visible range. Indeed, following the effective medium theory, a dense packing of such NPs should behave as a bulk homogenous medium characterized by a strong dispersion in its effective permittivity close to the plasmon resonance. On the long wavelength shoulder of the resonance, extremely high values of the effective permittivity are predicted, provided that the NPs are sufficiently densely packed. Such high values of the permittivity suggest that nanostructures formed from such dense NP composites, like the spherical cluster [18,19] depicted in Fig. 1, can support Mie-type resonances and act as magnetic dipoles at optical frequencies. Hence, by arranging such metaspheres into dense arrays, a metamaterial with a strong dispersion in its permeability, eventually reaching negative values, should be

#161083 - $15.00 USD Received 10 Jan 2012; revised 11 Feb 2012; accepted 11 Feb 2012; published 14 Feb 2012
(C) 2012 OSA

obtained. An important advantage of this method is that it offers the possibility to resort to bottom-up fabrication techniques based on colloidal self organization and should therefore allow an easy implementation of a bulk isotropic metamaterial with magnetic activity in the visible range.

In this contribution, we aim at exploring experimentally this approach in detail and introduce a novel fabrication strategy. As a first step, spectral properties of NPs composites with different filling fractions were experimentally characterized by ellipsometry and the effective permittivity of these materials was extracted. In a second step, NP metaspheres were fabricated using a method based on oil-in-water emulsions and their optical properties were investigated. Comparison of the experimentally measured extinction spectra to rigorous simulations clearly confirmed the excitation of a magnetic dipolar resonance at visible frequencies, demonstrating the potential of silver NPs for the bottom-up fabrication of isotropic magnetic metamaterials.

2. Effective permittivity of bulk silver nanoparticle composites

The resonant wavelength λ_r, at which the magnetic dipolar resonance of a dielectric sphere is excited, is essentially determined by the diameter d of the sphere and the permittivity ε_d of its constituent material. This resonance, which corresponds to the first order Mie mode, can be shown, following Mie scattering theory, to occur when the effective wavelength inside the dielectric tends to be comparable to the diameter of the sphere, e.g. when the following condition is fulfilled: $\lambda_r/\varepsilon_d^{1/2} \approx d$. The same condition applies for a NP metasphere by replacing ε_d with the effective permittivity of the NP composite or, in other words, by assuming that the NP assembly behaves effectively as an homogenous medium, as demonstrated in [14]. Hence, to determine under which conditions a NP cluster can sustain a magnetic resonance, it is essential to first determine the effective permittivity of the bulk NP composite from which the cluster is formed. It is well known from the Maxwell-Garnett (MG) effective medium theory that the effective properties of such a composite depends essentially on the density of NPs in the material. Therefore, prior to proceed to the fabrication of metal NP clusters, we first evaluated the dielectric constant of the NP composites used in this study as a function of their volume filling fractions using spectroscopic ellipsometry.

2.1 Methodology

Commercial dispersions of silver NPs (Harima Inc.) with an average diameter of 12 nm were used throughout this study. The localized plasmon resonance of the isolated NP appears as a strong peak around 400 nm in the absorption spectrum of dilute solutions (Fig. 2(a)). Note that silver was preferred over other metals due to its lower losses in the visible as indicated by the sharpness of the plasmonic peak. Furthermore, these inks, which are usually intended to be used for the fabrication of conductive patterns by inkjet printing, are provided at extremely high NP concentrations (typically more than 60%w), thanks to their hydrophobic coating which prevents their aggregation. This helped us to prepare (by dilution in the original solvent, tetradecane) several solutions covering a wide range of NP concentrations, from 0.0001 up to 10% vol., as estimated from the initial metal weight content and the NP size. To further increase the NP volume filling fraction, a thick dry film was prepared by spin coating the NP ink on a silicium substrate. By considering an average interparticle distance of 1-2 nm, as estimated from the TEM images (Fig. 2(a)), and a randomly close packed organization of the NPs, as shown by the SEM images (Fig. 2(b)), we estimated the NP volume filling fraction to be on the order of 30-40% in this film.

#161083 - $15.00 USD Received 10 Jan 2012; revised 11 Feb 2012; accepted 11 Feb 2012; published 14 Feb 2012
(C) 2012 OSA

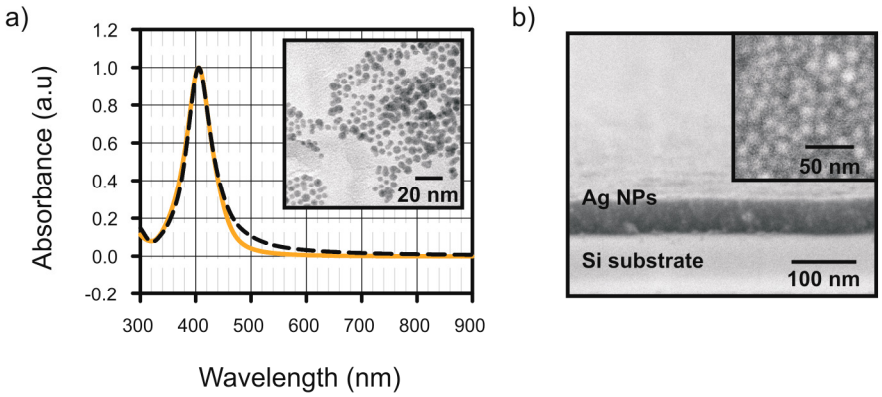

Fig. 2. (a) Experimental (plain) and calculated (dashed) absorption spectrum of the silver NP ink. Inset: TEM image of the silver NPs. (b) SEM image of the cross-section of a spin coated film of silver NPs. Inset: top view of the film.

The complex permittivities of these samples were measured with a standard variable angle spectroscopic ellipsometer (Jobin Yvon, UVISEL). The measurements were performed in reflection for the spectral range from 300 to 900 nm. The ellipsometric angles Δ and Ψ, which correspond respectively to the amplitude ratio and phase difference between the reflection coefficients for p and s polarized light, r_p and r_s, were recorded at various angles of incidence.. (55, 65 and 75°). The thickness and complex effective permittivity of the spin coated NP film were retrieved by fitting a two layer model (thin film plus substrate) to the experimental data. The dielectric constant of the film was modeled with a series of Lorentzian oscillators to account for the localized plasmon resonance as well as the 4d-5s interband transition of silver. The accuracy of the fit was checked by comparison with independent reflection spectra measurement and thickness analysis from SEM cross section and atomic force microscopy measurements. For the NP solutions on the other hand, the effective properties could be directly retrieved without the need of a model, by using a liquid cell with a frosted glass surface in order to minimize the reflection from the liquid/glass interface. As a result, only the air/liquid interface contributes to the reflected signals and the complex permittivity is directly retrieved from the measured complex reflectance ratio ρ, following the relation [23,24]:

$$\varepsilon_1 + i\varepsilon_2 = \sin^2\theta\left\{1+\left(\frac{1-\rho}{1+\rho}\right)^2\tan^2\theta\right\} \quad \text{with} \quad \rho = \frac{r_p}{r_s} = \tan\Psi e^{i\Delta}$$

Finally, the ellipsometry results were compared with predictions of the extended Maxwell Garnett (MG) effective medium theory [25,26] which relates the effective permittivity of the NP composite to the polarizability of the single NP as function of the NP filling fraction. The NP polarizability was calculated from Mie theory, considering 12 nm spherical silver NP surrounded by 2nm thick dielectric shell (ε = 2.6) and the dielectric constant of silver were taken from the literature [27] with a size dependant correction. The corresponding extinction spectrum, calculated with these parameters, is shown in Fig. 2(a).

2.2 Results and discussion

Figure 3(a) shows the dependence of the real and imaginary part of the permittivity on the volume fraction *f* occupied by the silver NPs in the different samples. In each case, a clear dispersion is observed in ε_1 with a dip and peak located respectively on the low and high wavelength side of the plasmon resonance, indicated by the peak in ε_2. These results show how both the absorption and dispersion spectrum of a silver NP composite can be altered by

#161083 - $15.00 USD Received 10 Jan 2012; revised 11 Feb 2012; accepted 11 Feb 2012; published 14 Feb 2012
(C) 2012 OSA

controlling the filling fraction of the NP, thereby giving access to a wide range of permittivity values. At low f (< 10^{-3}), the plasmon induced dispersion in ε_1 remains weak and the effective permittivity stays close to that of the host solvent (ε~2) over the whole visible range. As f is further increased, the dispersive shape gets more pronounced and shifts to higher wavelengths with ε_1 reaching negative values on the blue side of the plasmon resonance and a maximum value around 18 on the red side for the highest filling fraction considered here. Simultaneously, a strong red-shift and broadening of the plasmon peak is observed in the plot of ε_2 as f is increased. It is well known that this behavior results from the near field interactions between individual NPs which lead to the mixing of the individual resonances into collective modes. The progressive red-shift indicates the increase of the dipolar coupling strength as the average separation between NPs decreases. The minimum and maximum measured values of ε_1 are plotted as a function of f in Fig. 3(b), together with the calculated values from MG theory. There is an excellent agreement between the experimental and simulated data, suggesting that values of ε_1 close to 100 could be obtained by further increasing the density of NPs. These measurements can be used to predict the optical properties of specific structures fabricated from such NP composite like the spherical clusters that we are investigating. In this regard, it appears that only the highest filling fraction considered (f = 0.3-0.4) would provide a permittivity sufficiently high to induce a magnetic response in a subwavelength NP metasphere. Indeed, based on the value of ε_1 = 18 measured at λ = 580 nm, we can estimate that the smallest NP cluster which can support a magnetic Mie mode would have a diameter on the order of a hundred nanometers, as given by the formula $d = \lambda/\varepsilon_1^{1/2}$.

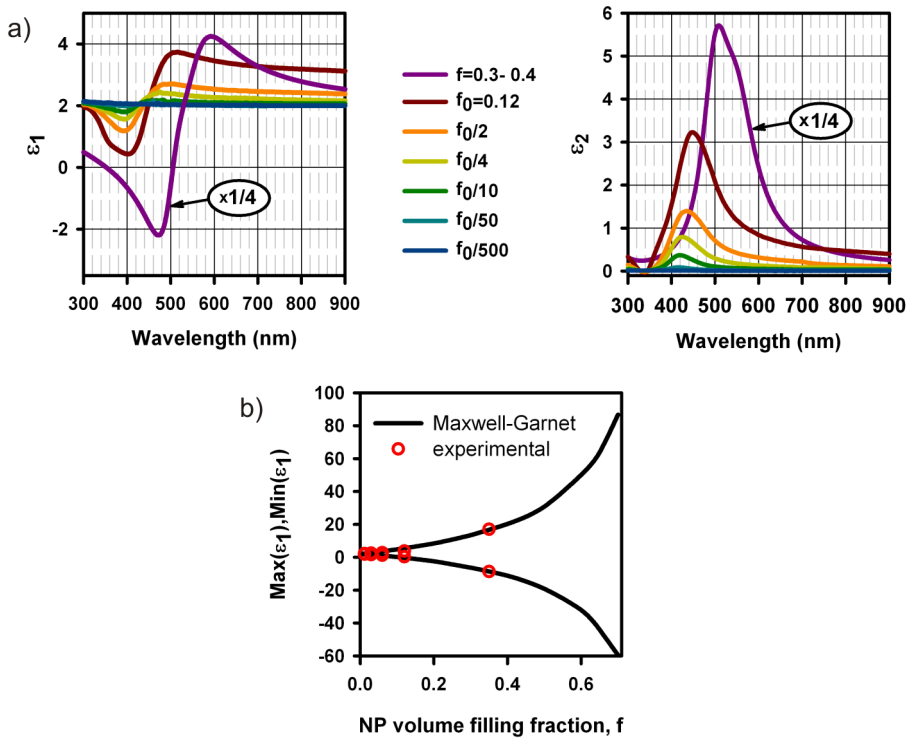

Fig. 3. (a) Real (left) and imaginary (right) part of the permittivity of silver NPs dispersed at different NP volume filling fractions f. For more clarity, the data obtained for the highest f (e.g. f = 0.3-0.4) have been divided by a factor 4. (b) Maximum and minimum values of the real permittivity as a function of the filling fraction as measured by ellipsometry (circle) and calculated from the Maxwell-Garnett formula (line).

#161083 - $15.00 USD Received 10 Jan 2012; revised 11 Feb 2012; accepted 11 Feb 2012; published 14 Feb 2012
(C) 2012 OSA

3. Silver nanoparticle metaspheres

3.1 Fabrication of spherical silver nanoparticle clusters

In order to fabricate NP clusters with the proper dimensions, we used a method inspired from the concept of oil-in-water emulsion. Similar approaches appear in the literature [28–30] for the fabrication of spherical clusters of NPs with different composition, including metallic ones, but little attention was given to their optical properties and in particular to their ability to sustain a magnetic dipole resonance. The idea of this method is to use emulsion droplets as nanocontainers to confine a discrete number of NPs. The aggregation of the encapsulated NPs is then induced in a second step by either evaporating the oil phase or adding a molecular linker (Fig. 4(a)). The size of the NP clusters is determined by the initial concentration of NPs in the oil phase and the size of the emulsion droplets which depends on the emulsification conditions (oil-to-water ratio, surfactant composition and concentration, and input agitation energy). In our case, 50 mL of the silver NP dispersed in tetradecane (1.2 $g.mL^{-1}$) were added drop-wise to 10 ml of an aqueous solution of polyvinylalcohol polymer (PVA Mw.9,000, 1%w), while simultaneously sonicating. PVA is widely used to form polymeric capsules, in particular in the field of medicinal chemistry for drug encapsulation. It acts as the emulsion stabilizer: the hydrophobic part of its polymeric chains arrange themselves at the surface of the oil droplets thereby lowering the interfacial tension between the two liquids and giving rise to steric stabilization forces which prevent the coalescence of the emulsion droplets.

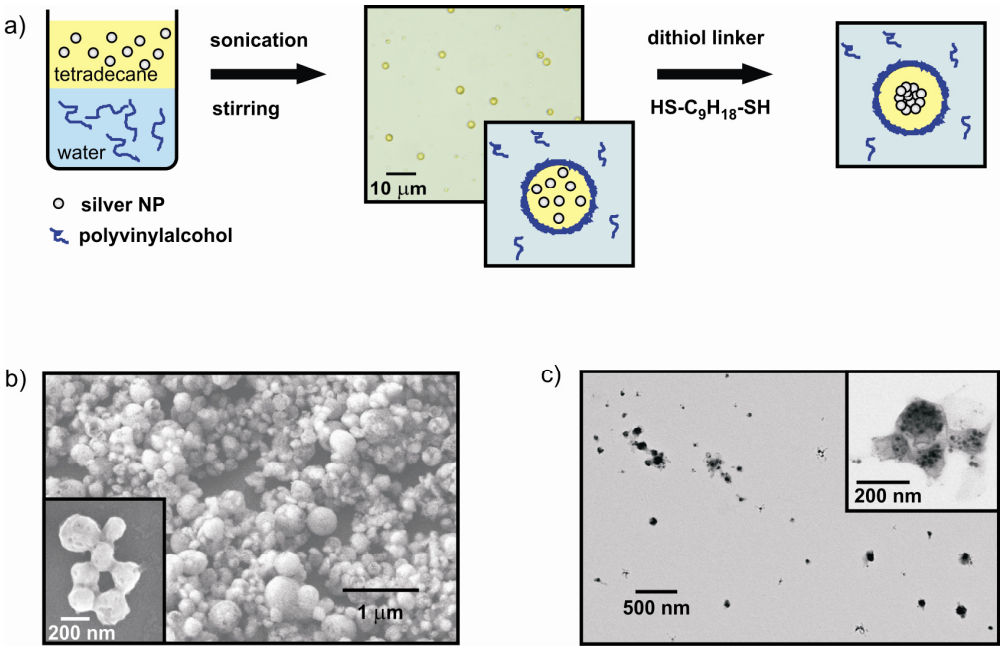

Fig. 4. (a) Sketch of the formation of spherical silver NP clusters in oil-in-water emulsions following the addition of a molecular dithiol linker. (b) SEM images of the raw emulsion showing the polymeric nanocapsules. (c) TEM images of the NP clusters.

Since the ink solvent, tetradecane, cannot be evaporated separately from the water continuous phase (due to its high boiling point and low vapour pressure), we introduced a dithiol linker to assemble the encapsulated silver NPs. A few drops (10 μL) of pure nonanedithiol was added right after the emulsification, giving a reddish colour, indicative of the NP aggregation, to the dark milky emulsion. The formation of spherical NP ink droplets in the continuous water phase was first confirmed by optical microscopy (Fig. 4(a)). To investigate the morphology of the polymeric capsules and the NP clusters, a few droplets of the raw emulsion were dried for SEM and TEM analysis. The SEM images clearly show the spherical PVA shell while the

#161083 - $15.00 USD Received 10 Jan 2012; revised 11 Feb 2012; accepted 11 Feb 2012; published 14 Feb 2012
(C) 2012 OSA

TEM micrographs confirm the presence of the silver NPs in the capsules and their agglomeration into clusters. We note however, that due to the high vacuum in the microscope chambers, the polymeric shells tend to break up. As can be seen from these images, the raw emulsion contain a broad size distribution of capsules, from a few tens of nms up to 500 nm approximately, corresponding to NP clusters with diameters up to 200 nm.

3.2 Optical properties

Prior to investigate the optical properties of these NP clusters, the emulsion was purified by filtration and the cluster size distribution was narrowed down by performing several cycles of centrifugation, collecting at each step the supernatant. The resulting fractions are characterized by a strong change of colour according to the different cluster sizes: from yellow for the smallest ones, to orange and purple for the biggest ones (Fig. 5(a), inset). The UV-Visible extinction spectra of the different fractions are shown in Fig. 5(a). The extinction spectra of the clusters are characterized by a strong extinction peak, strongly red-shifted in comparison with the single NP resonance (black curve) and shifting progressively to longer wavelengths as the cluster size increases, clearly suggesting the excitation of a collective resonance in the NP clusters. In order to gain more insight in the physical origin of these extinction peaks and to investigate their eventual relation to the excitation of a dipolar magnetic resonance, the experimental spectra were compared with rigorous simulations, based on the extended Mie theory [31,32]. This allows to calculate the overall optical response of an aggregate of interacting NPs. The simulated geometry consists in spherical clusters formed by an amorphous arrangement of 12 nm diameter silver NP with a fixed interparticle distance of 1.5 nm corresponding to the length of the dithiol linker (Fig. 5(b), inset). The cluster diameter, and hence the number of NPs, was varied between 40 to 150 nm (e.g. between 10 and 460 NPs) and the refractive index of the surrounding medium was set to 1.6 to match the experimental conditions.

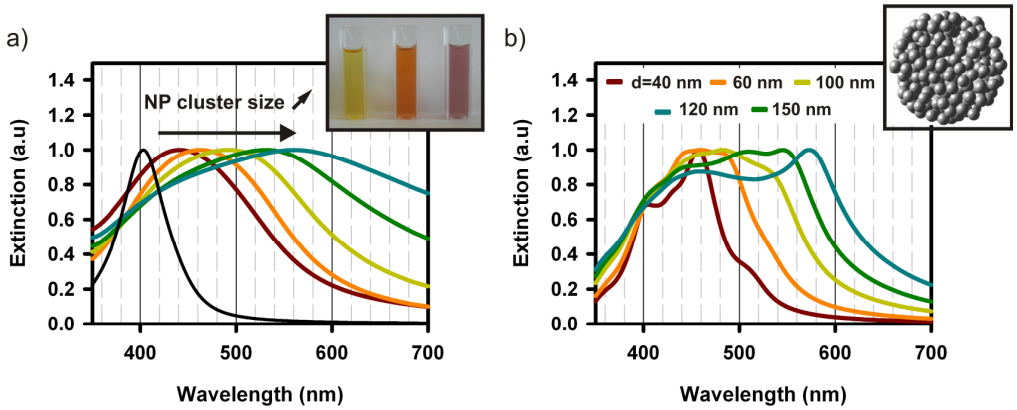

Fig. 5. (a) Experimental extinction spectra of the silver NP cluster dispersions for increasing cluster size. The black curve is the spectrum of isolated NPs. Inset: photo of the vials containing the NP clusters. (b) Simulated extinction spectra spherical silver NP clusters with different radiuses.

As can be seen in Fig. 5(b), the simulated extinction spectra show the same trends as the experimental spectra. In particular, the progressive red-shift when increasing the NP cluster diameter is well reproduced in the simulations, thereby confirming that the observed extinction peaks correspond to a collective resonance sustained by the entire clusters. On the other hand, the simulated spectra contain some fine structure below the main resonance which is not found in the measured spectra. These discrepancies are due to the fact that the simulation considers only an individual geometry whereas the clusters probed in the experiment, although characterized by similar shapes and sizes, exhibit different spatial

#161083 - $15.00 USD Received 10 Jan 2012; revised 11 Feb 2012; accepted 11 Feb 2012; published 14 Feb 2012
(C) 2012 OSA

arrangements of the NPs within them. The red-shifted resonance which is associated with the global shape of the clusters dominates the experimental spectra while the fine structure is related to the details of the NP arrangement inside the cluster and is smeared out in the experiment. Next, the simulated scattered field was related to the field radiated by a series of electric and magnetic multipoles through a multipole expansion [33–35]. In this way, the excitation of a magnetic dipole moment related to the observed resonance can be clearly identified. For all the diameters considered, the clusters are significantly smaller than the wavelength, hence only a few multipoles are expected to contribute to the total scattered field. Figure 6(a) shows the contribution of the magnetic dipole to the scattering cross-section. As can be seen, no magnetic dipole is excited for clusters having a diameter smaller than 100 nm. Their response is entirely described by an electric dipole contribution. On the other hand, a magnetic dipole contribution clearly emerges for larger diameters in the wavelength region corresponding to the red-shifted extinction peak. This is in good agreement with the rough estimation of the cluster size done in the previous section, based on the ellipsometric measurements. The contribution of this magnetic dipole grows significantly as the cluster size increases. To get a more complete description, the relative contribution of all the different excited multipoles from the simulation are shown for the cluster with the largest diameter in Fig. 6(b).

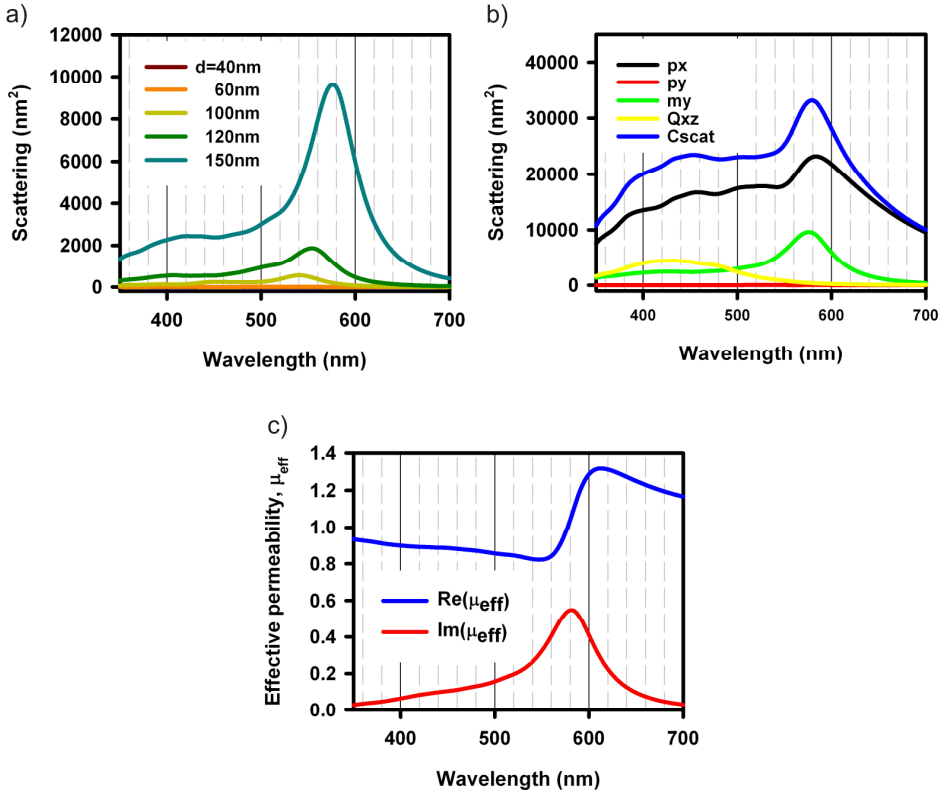

Fig. 6. (a) Contribution of the magnetic dipole moment to the scattering cross section of the NP cluster as a function of its radius. (b) Contribution of the various multipole moments (p, electric dipole; m, magnetic dipole; Q,electric quadrupole) to the scattering cross section for the larger cluster simulated (r = 75nm). The cluster was illuminated by a plane wave propagating along z direction with a polarization parallel to x direction. (c) Simulated effective permeability of a fcc arrangement of silver NP clusters ($f = 0.68$).

It can be seen that although the electric dipole still dominates the cluster's response, the magnetic dipole contributes significantly to the scattering cross section (by about 1/3). Since

#161083 - $15.00 USD Received 10 Jan 2012; revised 11 Feb 2012; accepted 11 Feb 2012; published 14 Feb 2012
(C) 2012 OSA

these results confirm the magnetic activity of the fabricated silver NP clusters, it is interesting to evaluate how this would be reflected in the effective permeability of a metamaterial formed by an arrangement of such clusters. This is done by inserting the magnetic polarizability of the cluster obtained from the previous calculations in the extended MG formula for the effective permeability μ [22]. The result is shown in Fig. 6(c) for a *cluster* filling fraction of 0.68 corresponding to close packed arrangement of clusters in a face-centered cubic lattice. A clear dispersion in the metamaterial permeability is observed around the cluster resonance, around 600 nm. Although this dispersion appears relatively weak with respect to the previous theoretical predictions [19], it compares well with the results recently obtained for gold NP clusters of slightly larger size [18] or for SiO2 spheres covered with a gold NP shell [20]. These results therefore demonstrate that the formation of metal NP clusters by emulsion and crosslinking offers an efficient way to realize magnetic meta-atoms. While their optical properties are similar to those previously reported [18,20], this original fabrication technique potentially expands the degrees of freedom available to tailor those properties and thereby their use in different applications. Several possibilities can be exploited to strengthen the magnetic response of the NP clusters. For instance, a further increase of the size of the clusters, by adjusting the emulsification conditions, should produce stronger resonances, as predicted by Mie theory. The size of the silver NP themselves could also be slightly increased, so as to reduce the losses due to confinement effects which still operate for 12 nm NPs. Alternatively, losses could also be reduced by introduce some gain medium, like organic dyes, in the emulsion process.

4. Conclusion

The present study investigates the potential of silver NPs for the bottom-up fabrication of optical metamaterials. First ellipsometric investigations showed that the dielectric constant of NP composites can be widely tuned in the visible region by controlling the NP filling fraction. In particular, high permittivity values were measured for densely packed NP arrangement, confirming the possibility to use such NP composite for the fabrication of magnetic meta-atoms. Such meta-atoms were prepared in the form of spherical NP clusters using a bottom-up technique based on emulsion technology. Their optical properties were carefully investigated by confronting their experimental UV-visible extinction spectra with rigorous simulations. The spectral response of the NP clusters is characterized by the appearance of a resonance, red shifting progressively when the cluster size is increased. While this resonance can be described as a pure electric dipole resonance for the smallest clusters, the excitation of a magnetic dipole was shown to contribute to the spectral response when the cluster size exceeds 100 nm. This magnetic response is induced by the strong permittivity of the NP medium and the spherical shape of the NP cluster. Using effective medium theories, it is further shown that this magnetic resonance can give rise to dispersion in the permeability of a metamaterial composed of an assembly of such clusters. Although these results clearly demonstrate the ability of silver NP clusters to act as magnetic meta-atoms, their magnetic activity remains relatively weak and further efforts will be necessary to strengthen their response.

Acknowledgments

This work was funded by the European Union's Seven Framework Programme (FP7/2007-2013) under grant agreement n°228455, by the Thuringian State Government (MeMa), and the German Federal Ministry of Education and Research (PhoNa).

#161083 - $15.00 USD Received 10 Jan 2012; revised 11 Feb 2012; accepted 11 Feb 2012; published 14 Feb 2012
(C) 2012 OSA